European Polymer Journal 67 (2015) 252–263

Contents lists available at ScienceDirect

European Polymer Journal

journal homepage: www.elsevier.com/locate/europolj

Chain-growth copolymerization of functionalized ethynylarenes with 1,4-diethynylbenzene and 4,4′-diethynylbiphenyl into conjugated porous networks

Sabina Stahlová [a], Eva Slováková [a], Petra Vaňkátová [a], Arnošt Zukal [b], Martin Kubů [b], Jiří Brus [c], Dmitrij Bondarev [d], Robert Moučka [e], Jan Sedláček [a,*]

[a] Department of Physical and Macromolecular Chemistry, Faculty of Science, Charles University in Prague, Hlavova 2030, CZ-128 43 Prague 2, Czech Republic
[b] J. Heyrovský Institute of Physical Chemistry, v.v.i., Academy of Sciences of the Czech Republic, Dolejškova 3, 182 23 Prague 8, Czech Republic
[c] Institute of Macromolecular Chemistry, v.v.i., Academy of Sciences of the Czech Republic, Heyrovský Sq. 2, 16206 Prague 6, Czech Republic
[d] Department of Polymer Engineering, Faculty of Technology, Tomas Bata University in Zlín, Vavrečkova 5669, 76001 Zlín, Czech Republic
[e] Centre of Polymer Systems, University Institute, Tomas Bata University in Zlín, Nad Ovčírnou 3685, 76001 Zlín, Czech Republic

ARTICLE INFO

Article history:
Received 2 February 2015
Received in revised form 21 March 2015
Accepted 29 March 2015
Available online 9 April 2015

Keywords:
Polyacetylenes
Diethynylbenzene
Diethynylbiphenyl
Conjugated networks
Microporous polymers
Rh-catalyst

ABSTRACT

We report the synthesis of conjugated highly cross-linked polyacetylene-type networks with a high content of functional groups (–CH_2OH, –NO_2, –Ph_2N, content up to 3.9 mmol/g) via a chain-growth copolymerization of either 1,4-diethynylbenzene or 4,4′-diethynylbiphenyl with functionalized mono- and diethynylbenzenes. The backbone of the networks consists of substituted polyene main chains that are cross-linked by arylene links. The optimized combinations of comonomers in the feed provide functionalized networks with a Brunauer–Emmett–Teller specific surface area up to 667 m^2/g and enhanced affinity for CO_2 adsorption (compared to the non-functionalized hydrocarbon networks of the same type). The dependence of the specific surface area of the networks on the size and architecture of the comonomers used for the synthesis is discussed in the paper. The reported networks can be classified into the group of conjugated microporous polymers (CMPs). Contrary to the CMPs synthesized by step-growth couplings, significantly lower average comonomer functionality in the feed (f = 1.5–2.0) is sufficient for the high specific surface area to be achieved in the reported polyacetylene-type CMPs.

1. Introduction

Microporous Organic Polymers (MOPs), *i.e.* polymers with permanent micro or micro/mesopores, have become a new class of porous materials over the last decade [1–5]. The potential applications of MOPs range from (i) gas separation and reversible storage [6–8], (ii) adsorption of chemicals [9,10], (iii) catalysis [11,12], (iv) energy transformation and storage [13,14] to (v) optoactive materials and sensors [15,16]. Except for polymers with intrinsic microporosity [17], the microporosity of MOPs results from the rigidity of the polymer segments combined with extensive cross-linking and/or hyperbranching [1–5].

Various classifications of MOPs have been applied in the literature [1–5]. If we adopt the source-based classification we can delimit an important subclass of MOPs derived from multifunctional ethynylarenes (MEAs), *i.e.* monomers containing usually from 2 to 4 terminal ethynyl groups attached to the arene core of the molecule. Polycyclotrimerization of MEAs with either $Co_2(CO)_8$ or $TaCl_5$ catalysts leads to hyperbranched, partially cross-

* Corresponding author. Tel.: +420 221951308.
E-mail address: jan.sedlacek@natur.cuni.cz (J. Sedláček).

http://dx.doi.org/10.1016/j.eurpolymj.2015.03.070
0014-3057/

linked polyarylenes, in which the original arene cores of monomers are interconnected by benzenetriyl linkers [18,19]. The MOPs with Brunauer–Emmett–Teller specific surface area, S_{BET}, up to 1547 m^2/g have been synthesized by this approach [11]. The palladium oxidative homo-coupling of MEAs results in microporous networks of the poly(arylenebutadiynylene) type [20,21]. The palladium Sonogashira cross-coupling of MEAs with di-, tri- and tetrahaloaromatics provides poly(aryleneethynylene) type networks [4,22]. The S_{BET} values around 500–1000 m^2/g are mostly reported for poly(arylenebutadiynylene) and poly(aryleneethynylene) MOPs [4] although exceptionally high values (S_{BET} 1700–1900 m^2/g) were reported for networks derived from tetrakis(4-ethynylphenyl)methane [23,24]. The "click" reaction of MEAs with di-, tri- and tetraazido aromatics is another path to MOPs (S_{BET} up to 1200 m^2/g) [23,25]. All the above listed polymerizations of MEAs proceed in a step-growth polymerization manner. The MOPs prepared by those reactions are, with respect to their π conjugated nature, often assigned to a broader group of conjugated microporous polymers (CMPs) [26].

Both hydrocarbon and heteroatom-containing (functionalized) MOPs derived from MEA are described in the literature [26] and the proper functionalization is reported as important factor for the achievement the desirable functional properties of these materials. For example, the functionalized MOPs have been reported that act as organocatalysts [27] or supports for anchoring organometallic [28] or metal [29] catalysts. The functionalization also modifies the efficiency and/or selectivity of MOPs in the adsorption of gases, vapors and solids (from solutions) [8,30–33]. In the case of MOPs formed by above mentioned azide-alkyne "click" chemistry the heteroatom-containing groups (triazole rings) are created due to the polymerization as network knots [23,25]. In other cases, functionalized MOPs are prepared via polymerization of properly functionalized MEA monomers [4,24,26]. The functionalized MOPs can be submitted to postpolymerization reactions and the character of the functionalization can be modified (*e.g.* conversion of amino groups to amido groups and other) [31,34]. The postpolymerization functionalization of hydrocarbon MOPs is also possible however it is used less often [35]. Significant progress in the synthesis of functionalized MOPs from MEAs was achieved especially when using the Sonogashira cross-coupling of functionalized monomers [4]. By this approach MOPs containing a variety of functional groups and moieties have been prepared ranging from MOPs with bipyridine [28] or imidazolinium [36] containing struts to MOPs functionalized with carboxyl [33] or hydroxy [30] groups (for a comprehensive overview see Ref. [4]). It should be noted that the functionalization of MOPs is often accompanied by partial deterioration of the specific surface area in comparison to that of the hydrocarbon MOPs counterparts. This was well demonstrated by Cooper et al. in the comparative study dealing with MOPs synthesized by Sonogashira cross-coupling of 1,3,5-triethynylbenzene and functionalized dibromoarenes (functional groups: F, NO_2, OH, OMe, COOMe, CF_3, NH_2) [30].

Recently we have reported a transformation of 1,4-diethynylbenzene, 1,3-diethynylbenene and 4,4′-diethynylbiphenyl into hydrocarbon conjugated MOPs via a new method consisting in the one step chain-growth homopolymerization of these monomers into cross-linked polyacetylene type networks (Scheme 1) [37]. This reaction was far more facile route to the polyacetylene networks than the three step approach reported by us earlier [38]. We have optimized the catalyst for the one step polymerization: from Rh, W and Mo compounds known as active catalysts in phenylacetylene polymerizations [39,40] only Rh catalysts (particularly [Rh(nbd)acac] complex, nbd = norborna-2,5-diene, acac = acetylacetonato) were efficient in transformation of the above diethylarenes into porous networks [41]. The texture of prepared networks was found to be sensitive to the reaction conditions: prevailingly microporous products (S_{BET} up to 880 m^2/g) resulted from the polymerizations at room temperature while micro/mesoporous products (S_{BET} up to 1470 m^2/g) were obtained at 75 °C, particularly if the reaction time was prolonged [41]. The application of the HIPE (High Internal Phase Emulsion) approach to the Rh catalyzed polymerization of 1,3-diethynylbenzene provided products with hierarchically structured micro/macroporous morphology (walls of the macropores were formed by the microporous polymer) [42]. As evident from Scheme 1, the polyacetylene networks contain some amounts of non-transformed terminal ethynyl groups. We used them for the postpolymerization functionalization of the networks via the azide-alkyne "click" chemistry. However, only a low to moderate extent of the "click" reaction was attained [42].

In this article we report the synthesis of porous polyacetylene networks with high contents of functional groups via Rh catalyzed chain-growth copolymerization of hydrocarbon and functionalized ethynylarenes. The functionalized monomers with various functional groups and molecular architecture and the hydrocarbon diethynylarenes differing in the length of the spacer between ethynyl groups have been used for the synthesis. The influence

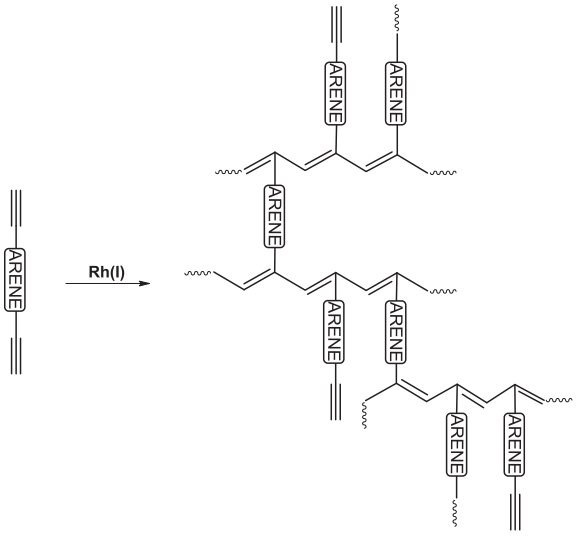

Scheme 1. Chain growth homopolymerization of diethynylarenes into hydrocarbon polyacetylene networks.

of these parameters on N_2 and CO_2 adsorption on the resulting networks is discussed.

2. Experimental part

2.1. Materials

1,4-Diethynylbenzene (DEB) (Sigma Aldrich) was purified by vacuum sublimation, 4,4′-diethynylbiphenyl (DEBPh) (TCI Europe), 1-ethynyl-4-nitrobenzene (M1) (Sigma Aldrich), 1-ethynyl-4-(hydroxymethyl)benzene (M2) (Sigma Aldrich), 1-ethynyl-4-(diphenylamino) benzene (M3) (TCI Europe), 1,3-diethynyl-5-nitrobenzene (M4) (Spectra Group Limited, Inc.), and acetylacetonato (norborna-2,5-diene)rhodium(I) [Rh(nbd)acac] (Sigma Aldrich) were used as obtained. Dichloromethane (Lachema, Czech Republic) was distilled from P_2O_5.

2.2. Polymerizations

All the chain-growth homo and copolymerizations were catalyzed by [Rh(nbd)acac] complex and were performed in CH_2Cl_2 at room temperature. The reaction time was 3 h. The initial concentrations were: $[Catalyst]_0$ = 18 mmol/L, the overall concentration of comonomers = 0.6 mol/L. Copolymerization of M1 with DEB is described as a typical example: 221 mg (1.5 mmol) of M1 and 189 mg (1.5 mmol) of DEB were placed in a screw cap vial and dissolved in 4 mL CH_2Cl_2. Then a solution of 26 mg of [Rh(nbd)acac] (0.09 mmol) in 1 mL CH_2Cl_2 was added into the solution of the monomers under stirring, which started the copolymerization. After 3 h, the precipitated polymer was separated, washed repeatedly by CH_2Cl_2 (100 mL CH_2Cl_2 altogether), and dried in vacuum at room temperature. The yield of copolymer was determined gravimetrically.

2.3. Techniques

All the Fourier transform IR (FTIR) spectra were measured on a Nicolet Magna IR 760 using the diffuse reflection mode (DRIFT). Samples were diluted with KBr.

All the ^{13}C cross-polarization magic-angle spinning (CP/MAS) NMR spectra were measured using a Bruker Advance 500 WB/US NMR spectrometer in a double-resonance 3.2 mm probehead at a spinning frequency of 20 kHz, as described previously [37].

Diffuse reflectance (DR) UV–vis spectra of polymers were recorded using a Perkin–Elmer Lambda 950 spectrometer. The polymers were diluted with $BaSO_4$ (1/10, w/w) before the measurements were carried out.

Elemental analyses of the polymers were done at the Institute of Macromolecular Chemistry, Academy of Sciences of the Czech Republic.

Nitrogen adsorption/desorption isotherms on the polymers were measured at 77 K using a Gemini II 2370 volumetric surface area analyzer (Micromeritics). Prior to the sorption measurements, all samples were degassed on a Micromeritics FlowPrep060 instrument under helium flow at 383 K for 8 h.

Adsorption isotherms of carbon dioxide on selected polymers were recorded at 273 K using an ASAP 2020 (Micromeritics) volumetric instrument. The samples were degassed at 383 K for 8 h under turbomolecular pump vacuum. Since the adsorption isotherms of CO_2 on organic polymers can depend on the time allotted to the adsorption measurement [19], all the isotherms were recorded using the same equilibration time interval of 5 s (the equilibration time interval represents the number of seconds between successive pressure readings during equilibration). The temperature of the sample was maintained with an accuracy of ±0.01 K using an Iso-Therm thermostat (e-Lab Services, Czech Republic).

Thermogravimetric analysis (TGA) was performed on a TA Q500 apparatus under nitrogen atmosphere with a heating rate of 10 °C min^{-1} in the range from 40 to 800 °C. The samples were treated at 100 °C for 60 min under nitrogen flow prior to analysis to remove trapped moisture.

Broadband dielectric spectroscopy measurements were carried out using an impedance analyzer (Novocontrol Concept 50, Germany) in a broad frequency and temperature range; 0.1 Hz to 1 MHz and −150 to 80 °C, respectively, with the measuring voltage amplitude equal to 1 V. Scanning Electron Microscopy was performed on Vega II/LMU (Tescan, Czech Republic) apparatus equipped with a backscattered electron (BSE) detector, secondary electron (SE) detector, and an energy dispersive X-ray (EDX) analyzer INCA (Oxford Instruments, UK).

3. Results and discussion

3.1. Functionalized polyacetylene networks by copolymerization of mono- and diethynylarenes

The Rh(I) complexes with cyclodiene ligands are highly efficient catalysts for the chain-growth polymerization of ethynylarenes with one terminal ethynyl group into linear conjugated polyacetylene-type polymers [39,43,44]. The catalysts exhibit high polymerization selectivity, so that the extent of cyclotrimerization of monomers into trisubstituted benzenes (that might be assumed to accompany the polymerization) is either very low or undetectable. Previously, we have reported the application of these catalysts, [Rh(nbd)acac] complex in particular, for the chain-growth polymerization of the hydrocarbon diethynylarenes into conjugated microporous polyacetylene-type networks (Scheme 1) [37,41]. These networks contain: (i) branching units (when both ethynyl groups of the monomer molecule react) and (ii) linear units (when only one ethynyl group of the monomer molecule reacts). The content of the latter units is from 35% to 70%, depending on the polymerization conditions. A (partial) replacement of these units by linear units with a heteroatomic functional group that would be achieved under preservation of the microporous character of the networks is, unambiguously, an interesting challenge. In this chapter, we report on the achievement of this goal through copolymerization of hydrocarbon bifunctional monomers with monofunctional monomers bearing a heteroatomic group according to

Scheme 2. 1,4-Diethynylbenzene (DEB) and 4,4′-diethynylbiphenyl (DEBPh) that differ in the length of the arylene spacer between ethynyl groups were used as bifunctional monomers. Three *para*-substituted phenylacetylenes (PAs), M1, M2, and M3 were selected as monofunctional monomers owing to the good compatibility of their functional groups with polymerization catalyst. The formulas and codes of the monomers are given in Scheme 2. The mole ratio of bifunctional to monofunctional monomers in the feed was 1:1; consequently, the average monomer functionality in the feed, *f*, was 1.5. Moreover, the DEB and DEBPh monomers were homopolymerized into non-functionalized hydrocarbon networks under the same conditions. For more detail on the experimental procedure, see Section 2. The results of the polymerization and codes of the polymers are summarized in Table 1. The homopolymerizations of DEB and DEBPh provided high yield of the polymers P(DEB) and P(DEBPh), respectively (see Table 1). Similarly, high polymer yields were achieved in the copolymerizations of DEBPh with M1, M2, and M3 (85–92%). On the other hand, if DEB (*i.e.*, a monomer with a short spacer between ethynyl groups) was used for the copolymerization, the copolymer yields were lower (66–77%).

All polymers of Table 1 were insoluble in tested solvents (THF, CH_2Cl_2, $CHCl_3$, benzene, DMF, and DMSO). The ^{13}C CP/MAS NMR spectra of the polymers of Table 1 are shown in Figs. 1 and 2 (for FTIR spectra, see Supplementary Data). In general, the ^{13}C CP/MAS NMR spectra contain signals at about $\delta = 83$ ppm and $\delta = 76$ ppm, which correspond to the resonance of sp carbons of non-transformed pendant ethynyl groups of monomeric units derived from DEB or DEBPh and a broad, partially resolved signal in the region 115–150 ppm that corresponds to sp^2 carbons of aromatic rings and polymer main-chains. The heteroatomic functional groups are manifested in the ^{13}C CP/MAS NMR spectra of the copolymers as follows: (i) the spectra of P(DEB/M2) and P(DEBPh/M2) contain a signal at $\delta = 64$ ppm due to the sp^3 carbons of CH_2OH groups, and (ii) the spectra of P(DEB/M1), P(DEBPh/M1), P(DEB/M3), and P(DEBPh/M3) comprise a partially resolved signal at $\delta = 147$ ppm due to the quaternary aromatic carbons bonded to the nitrogen of either nitro (M1) or amino (M3) groups.

The ^{13}C CP/MAS NMR spectroscopy indicates that the copolymers of Table 1 contain three kinds of monomeric units (see Scheme 2): (i) branching non-functionalized units (BN) derived from DEB or DEBPh, (ii) linear non-functionalized units (LN) derived from DEB or DEBPh, and (iii) linear functionalized units (LF) derived from functionalized PA-type monomers. The DEB and DEBPh homopolymers contain the BN and LN type units only. The mole fractions

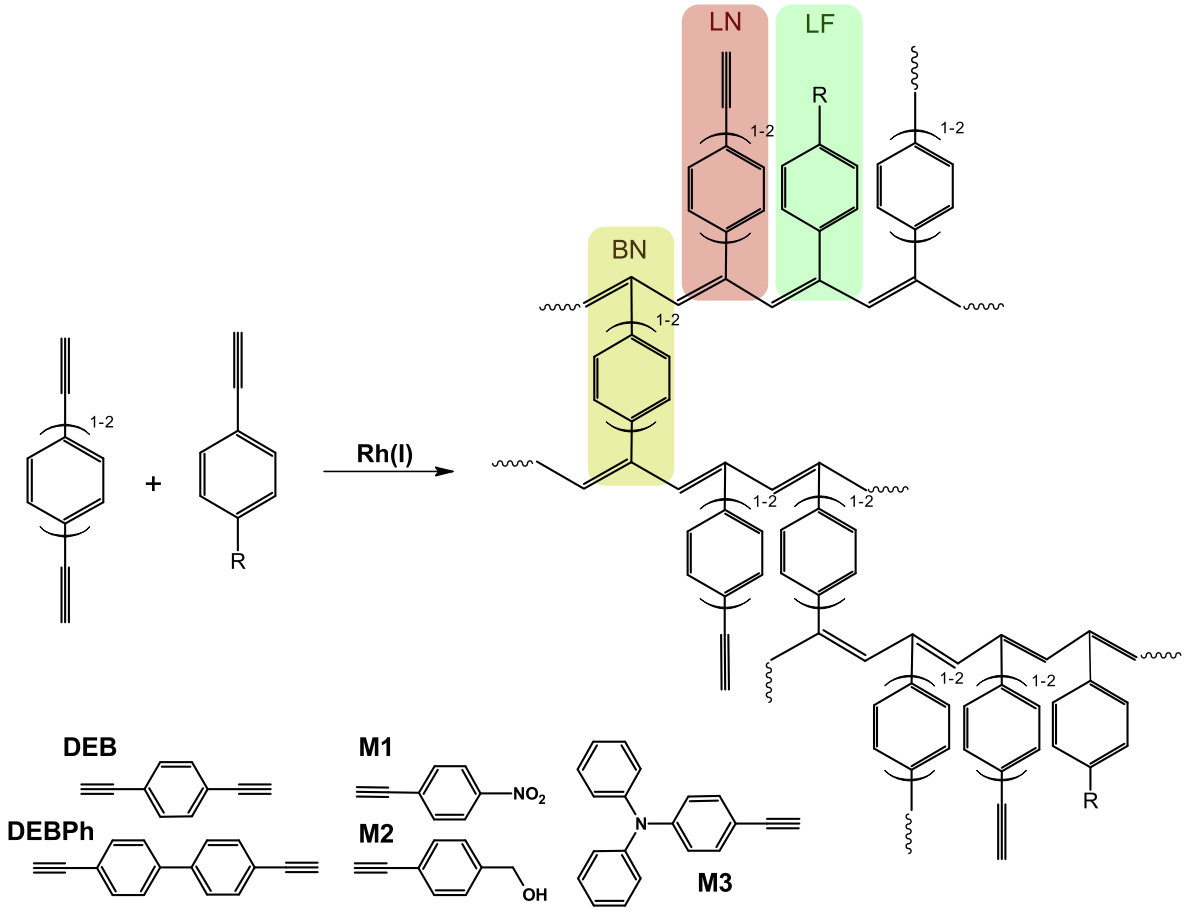

Scheme 2. Chain growth copolymerization of diethynylarenes with functionalized phenylacetylenes into functionalized polyacetylene networks.

Table 1
Copolymerization of functionalized phenylacetylenes (M1, M2, M3) with DEB or DEBPh and homopolymerization of DEB and DEBPh. *Y* is the polymer yield, ζ is degree of conversion of pendant ethynyl groups of DEB or DEBPh monomeric units, x_{BN}, x_{LN} and x_{LF} stand for the mole fraction of respective monomeric units (Scheme 2), $c_{(FG)}$ is the content of heteroatomic functional groups in copolymers in mmol/g. S_{BET} is the specific surface area, V_T is the total pore volume at $p/p_0 = 0.95$ and $V_{0.1}$ is the pore volume at $p/p_0 = 0.10$ (all from the N_2 adsorption isotherms).

Polymer Code	Monomers	*Y* (%)	ζ	x_{LF}	x_{LN}	x_{BN}	$c_{(FG)}$ (mmol/g)	S_{BET} (m^2/g)	$V_{0.1}$ (cm^3/g)	V_T (cm^3/g)
P(DEB)	DEB	96	0.36	0.00	0.64	0.36	0	882	0.32	0.78
P(DEB/M1)	DEB + M1	69	0.54	0.50	0.23	0.27	3.7	141	0.05	0.16
P(DEB/M2)	DEB + M2	77	0.36	0.50	0.32	0.18	3.9	239	0.09	0.35
P(DEB/M3)	DEB + M3	66	0.08	0.36	0.60	~0.05	2.0	2	–	–
P(DEBPh)	DEBPh	92	0.61	0.00	0.39	0.61	0	604	0.23	0.47
P(DEBPh/M1)	DEBPh + M1	90	0.64	0.45	0.20	0.35	2.5	429	0.17	0.42
P(DEBPh/M2)	DEBPh + M2	85	0.50	0.50	0.25	0.25	3.0	459	0.17	0.58
P(DEBPh/M3)	DEBPh + M3	92	0.62	0.50	0.19	0.31	2.1	1	–	–

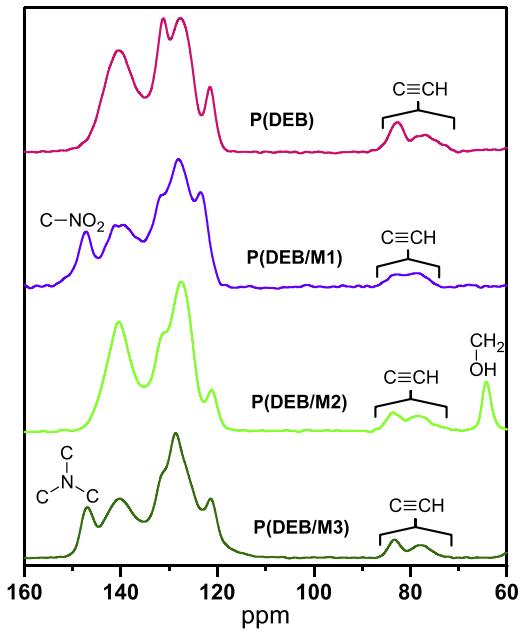

Fig. 1. ^{13}C CP/MAS NMR of DEB series of polymers of Table 1.

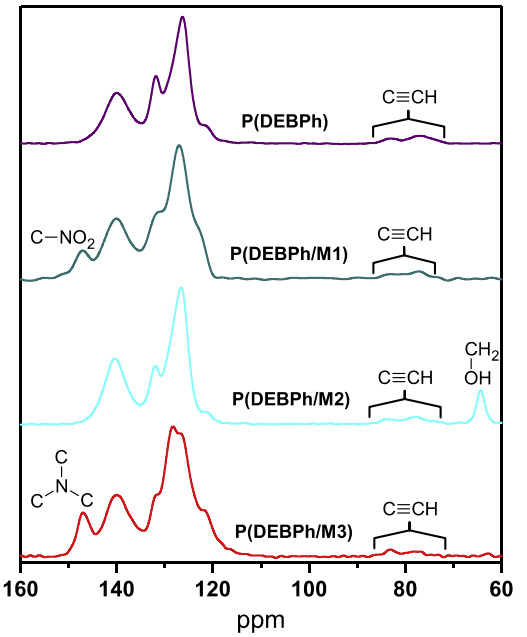

Fig. 2. ^{13}C CP/MAS NMR of DEBPh series of polymers of Table 1.

of individual units in the polymers (x_{BN}, x_{LN}, and x_{LF}) are summarized in Table 1. The mole fractions of nitrogen containing LF units were determined on the basis of the nitrogen content in respective copolymers given by the elemental analysis (see Supplementary Data). The mole fractions of LF units with CH_2OH groups in P(DEB/M2) and P(DEBPh/M2) and the values of x_{BN} and x_{LN} in all polymers were determined form the ^{13}C CP/MAS NMR spectra (Figs. 1 and 2) [37].

The values of x_{LF} of all copolymers of Table 1, except for P(DEB/M3), lie in the interval from 0.45 to 0.5; *i.e.*, they are (roughly) equal to the mole fraction of the PA-type monomers in the feeds. Evidently, the incorporation of PA-type monomers into the networks proceeded smoothly despite their lower functionality ($f = 1$) compared to that of DEB and DEBPh ($f = 2$). The incorporation of a PA-type monomer into the copolymer was less efficient only in the case of the P(DEB/M3) copolymer, for which x_{LF} of 0.36 was attained (Table 1).

By analogy with the chain-growth (co)polymerization of divinyl-type monomers described in the literature [45,46] one can assume that the molecules of bifunctional monomers (DEB, DEBPh) are incorporated into (co)polymer chains as linear monomeric units with pendant ethynyl groups at the early beginning of the polymerizations. Subsequently, some pendant ethynyl groups participate in the polymerization, which ultimately leads to the cross-linking of chains. The degree of conversion of pendant ethynyl groups in the polymers of Table 1, ζ, can be defined as follows: $\zeta = x_{BN}/(x_{BN} + x_{LN})$ (see Table 1 for the values of ζ). The quantity ζ is equal to x_{BN} in the case of DEB and DEBPh homopolymers. In the case of copolymers of Table 1, the $\zeta > x_{BN}$, since the units derived from a bifunctional monomer (BN and LN) are diluted with units derived from a monofunctional monomer (LF) in the copolymer chains. All the copolymers of Table 1, except for P(DEB/M3), exhibit similar values of ζ as the respective DEB and DEBPh homopolymers. This means that the transformation of the pendant ethynyl groups of DEB or DEBPh monomeric units is not negatively affected by the presence of LF units in the chains of these copolymers. Nevertheless,

the extent of cross-linking of these copolymers (which is assumed to be proportional to the x_{BN} values) is lower compared to the extent of cross-linking of the respective DEB and DEBPh homopolymers just due to the "dilution" of the branching units in the copolymers by LF units. A sample of P(DEB/M3) exhibits ζ and x_{BN} values of only 0.08, and 0.05, respectively; *i.e.*, most pendant ethynyl groups of DEB monomeric units remain non-reacted in this copolymer. Most probably, the bulky 4-(diphenylamino)phenyl substituents sterically restrict the access of ethynyl groups of linear 4-ethynylphenyl-substituted units to the polymerization active centers.

The dielectric properties of polymers from Table 1, except for P(DEB/M3) and P(DEBPh/M3), were investigated by means of broadband dielectric spectroscopy (DS) on the samples compressed into the shape of compact pellets (see Section 2). In the case of P(DEB/M3) and P(DEBPh/M3), the compression was not feasible due to the sample microstructure. The samples were investigated in the temperature range from −150 to 80 °C and frequency range from 0.1 Hz to 1 MHz. All the samples exhibited no substantial change in the real part of permittivity. This indicates a restricted mobility of larger polymer segments due to the extensive cross-linking, which corresponds to the covalent structure proven by ^{13}C CP/MAS NMR. Nevertheless, relaxations of various intensities were detected in the imaginary part of permittivity (see Fig. 3).

The homopolymer P(DEB) exhibits weak relaxation at low-temperature, which is attributable to the γ relaxation of 4-ethynylphenyl pendant groups. This relaxation is considerably weaker in the P(DEBPh) homopolymer most probably due to the high extent of cross-linking of P(DEBPh) (x_{BN} = 0.61, Table 1). On the other hand, intensive γ relaxation accompanied by β relaxation (at elevated temperature) was revealed in the case of copolymers with CH_2OH groups [P(DEB/M2) and P(DEBPh/M2)]. This reflects (i) the presence of polar hydroxyl groups in the copolymers and (ii) the low extent of cross-linking of these copolymers. Surprisingly, copolymers with NO_2 groups [P(DEB/M1) and P(DEBPh/M1)] exhibit less pronounced γ and β relaxations despite the fact that NO_2 groups carry higher dipole moment and hence contribute more to the polarization of pendant groups than CH_2OH groups (compare the dipole moments of nitrobenzene, 4.42 D, and (hydroxymethyl)benzene, 1.71 D). Restricted mobility of nitrophenyl pendants due to (i) the higher extent of cross-linking (Table 1) and/or (ii) the tighter packing of segments in copolymers comprising NO_2 groups may explain this finding. The activation energy, extracted from Arrhenius temperature behavior, of relaxations at low-temperature region was accessible for P(DEB/M1), P(DEB/M2), and P(DEBPh/M2) copolymers with values in the range from 40 to 60 kJ/mol (see Supplementary Data), which supports the ascription of these relaxations to γ relaxation processes.

All the copolymers of Table 1 were characterized by N_2 adsorption at 77 K. The N_2 adsorption/desorption isotherms on samples of DEBPh series are shown in Fig. 4; the respective isotherms on the samples of the DEB series are in Supplementary Data.

Both copolymers containing monomeric units derived from M3, P(DEB/M3) and P(DEBPh/M3), adsorbed only negligible amounts of N_2. The values of (i) the Brunauer-Emmett-Teller specific surface area, S_{BET}, (ii) the total pore volume at p/p_0 = 0.95, V_T, and (iii) the pore volume at p/p_0 = 0.10, $V_{0.1}$, ascertained from the N_2 adsorption isotherms are summarized in Table 1. All the copolymers exhibited lower S_{BET} values as compared to P(DEB) and P(DEBPh) homopolymers. A decrease in S_{BET} due to the functionalization was also reported by Cooper et al. in the case of poly(aryleneethynylene) microporous networks [30]. In our case, the S_{BET} value of P(DEB/M1) and P(DEB/M2) copolymers dropped to 16% and 27% of the S_{BET} value of P(DEB) homopolymer. Much better relation was obtained for the DEBPh sample series: the S_{BET} values of P(DEBPh/M1) and P(DEBPh/M2) copolymers represented about 70–75% of the S_{BET} value of the P(DEBPh) homopolymer (see Table 1). The values of $V_{0.1}$, which roughly represent the micropore volume of the polymers [30], exhibited the same trends as those outlined above for the S_{BET} values. The values of V_T are contributed (in addition to the micropore volume) by the volume of mesopores and, possibly, by the interparticle void volume. Previously, we have reported the formation of mesopores in DEB homopolymers and suggested that they may be formed via interconnection of microporous polymeric particles in the late stage of polymerization [41]. The inspection of the V_T and $V_{0.1}$ data in Table 1 shows that copolymers containing M2 monomeric units most probably exhibit the highest percentage contribution of mesopore volume to the total pore volume. This is in accordance with the shape of N_2 adsorption isotherms on P(DEB/M2) and P(DEBPh/M2), which shows the most pronounced N_2 trapping at higher relative pressures.

Summarizing this chapter, we can state that the copolymerization according to Scheme 2 can produce functionalized micro/mesoporous networks. In our case, the porosity of the networks seems to be affected mainly by the ratio of the size of (i) the pendant group of a monofunctional monomer and (ii) the linker of a bifunctional monomer. If the pendant group of a monofunctional monomer is considerably larger than the linker of the bifunctional monomer (combination of DEB and M3 monomers), the cross-linking is not sufficient, and the resulting copolymer is, of course, nonporous. Nevertheless, even if a high extent of cross-linking is achieved, the copolymer porosity is not obvious in all cases. A combination of DEBPh and M3 gives a highly cross-linked but nonporous copolymer. One can especially assume that the bulky 4-(diphenylamino)phenyl substituent of M3 occupies the potential pore volume in the network in this case. On the other hand, a satisfactory porosity is achieved in copolymers prepared from pairs of monomers in which the linker of the bifunctional monomer is larger in size than the pendant group of the monofunctional monomer (DEBPh + M1 and DEBPh + M2 combinations). If monomers of a similar size of the linker and pendant group are combined into copolymers (combinations DEB + M1 and DEB + M2), the porosity and corresponding S_{BET} is considerably reduced. Several effects may contribute to this finding: (i) the low extent of cross-linking of P(DEB/M1) and P(DEB/M2) (Table 1), (ii) steric effects of the NO_2 and $HOCH_2$ groups of M1 and M2 (although the size of these groups is not large, it might play

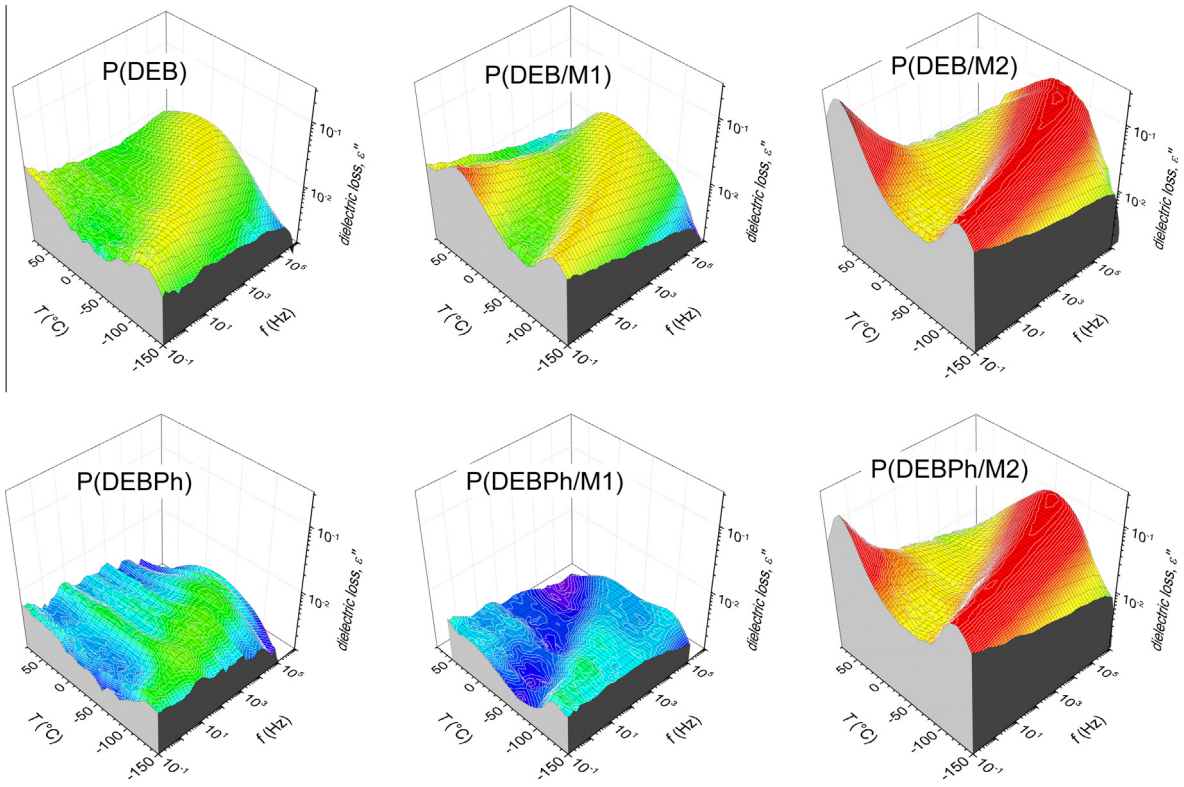

Fig. 3. Frequency and temperature dependencies of the dielectric loss for selected samples of Table 1.

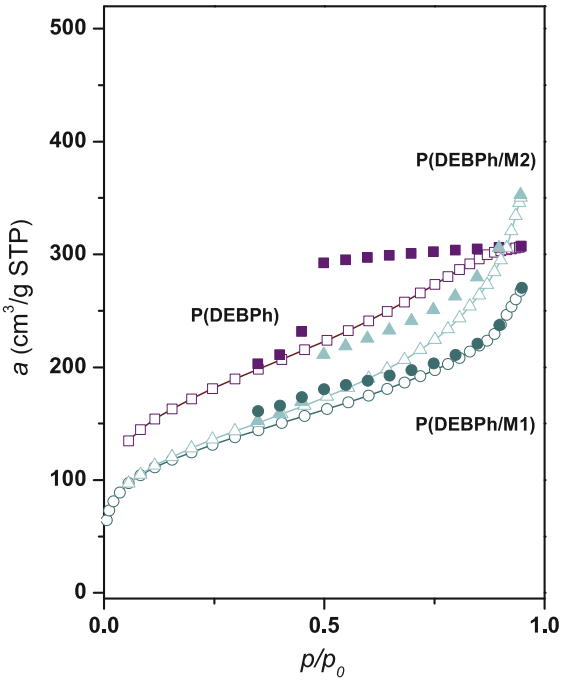

Fig. 4. N_2 adsorption isotherms on microporous polymers of the DEBPh series of Table 1.

a role in the networks cross-linked via small DEB units), and (iii) a possible electronic interaction between polar NO_2 or $HOCH_2$ groups and surrounding polymer moieties that may lead to a tighter packing of the polymer segments or a partial collapse of the microporous polymer texture. It should also be noted that the content of NO_2 and $HOCH_2$ functional groups ($c_{(FG)}$ in mmol/g) is higher in the copolymers of DEB series (3.7 and 3.9 mmol/g, respectively) than in the copolymers of DEBPh series (2.5 and 3.0 mmol/g, respectively). That is why the effects (ii) and (iii) may be more pronounced in P(DEB/M1) and P(DEB/M2) than in P(DEBPh/M1) and P(DEBPh/M2).

3.2. Functionalized polyacetylene networks derived from 1,3-diethynyl-5-nitrobenzene

1,3-Diethynyl-5-nitrobenzene (M4) is a monomer that comprises both (i) a heteroatomic group and (ii) two ethynyl groups in one molecule. M4 was introduced in the polymerization described in this chapter with the aim to enhance the extent of functionalization and/or cross-linking of the resulting networks. The homopolymerization of M4 provided high yield of insoluble P(M4) network containing one NO_2 group per each monomeric unit (Table 2). ^{13}C CP/MAS NMR spectroscopy (Fig. 5) confirmed the presence of both linear units, LF, ($x_{LF} = 0.52$) and branching units, BF, ($x_{BF} = 0.48$) in P(M4). Despite the high extent of cross-linking of P(M4), the S_{BET} of 16 m^2/g only was revealed by N_2 adsorption on this network (see Fig. 6 for the N_2 adsorption isotherm). Both steric and electronic effects (*vide supra*) of NO_2 groups that are present in high concentration in P(M4) ($c_{(FG)} = 6.5$ mmol(NO_2)/g) may be responsible for the lack of the porosity of P(M4).

The high yield of networks also resulted in copolymerization of M4 with either DEB or DEBPh (the mole ratio of the comonomers in the feed is 1:1, $f = 2$, see Table 2 and Scheme 3). It can be assumed that the copolymers of Table 2 contain, in addition to the LF and BF units derived from M4, linear (LN) and branching (BN) units derived from DEB or DEBPh monomers. The combination of ^{13}C CP/MAS NMR spectroscopy (Fig. 5) and elemental analysis (Supplementary Data) allowed one to ascertain only the total mole fraction of the nitro group containing units in the copolymers ($x_{LF} + x_{BF}$) and the total fraction of the branching units in the copolymers ($x_{BN} + x_{BF}$). Both copolymers of Table 2 have a comonomeric composition close to that of the feed ($x_{LF} + x_{BF} = 0.45$, the mole fraction of M4 in the feed = 0.5). The total fraction of branching units in the copolymers of Table 2 is about 0.5; *i.e.*, it is higher than that achieved for the NO_2 group containing copolymers of Table 1. The enhancement of the functionality of comonomers in the feed from $f = 1.5$ (Table 1) to $f = 2$ (Table 2) results in an increase in the extent of cross-linking. The copolymers of Table 2 exhibit S_{BET} values of 667 m^2/g [P(DEB/M4)] and 414 m^2/g [P(DEBPh/M4)], which are significantly higher than the S_{BET} value of P(M4) homopolymer of the same extent of cross-linking. Unambiguously, the dilution of NO_2-functionalized M4-based units by hydrocarbon units ($c_{(FG)} = 2.4–3.1$ mmol(NO_2)/g) positively affects the porosity of M4-based networks.

The data of Tables 1 and 2 allow one to compare the specific surface area of three NO_2-functionalized networks constructed from monomers with benzene cores and differing in the fraction of branching units and the content of NO_2 groups. The S_{BET} value of these polymers increases in the series: P(M4) (16 m^2/g, 0.48, 6.5 mmol/g) ≪ P(DEB/M1) (141 m^2/g, 0.27, 3.7 mmol/g) < P(DEB/M4) (667 m^2/g, 0.55, 3.1 mmol/g); the S_{BET} values, the fraction of branching units, and the NO_2 group content, respectively, are given in the parenthesis behind the polymer codes. As evident, both the fraction of branching units and the content of NO_2 groups are important for the S_{BET} value of the networks of this series: a too high content of NO_2 groups [P(M4)], as well as a low extent of cross-linking [P(DEB/M1)], deteriorate the S_{BET} values.

3.3. CO_2 adsorption on prepared polymers

The networks from Tables 1 and 2 with $S_{BET} > 400$ m^2/g were investigated as to their CO_2 adsorption efficiency at 273 K. Fig. 7 shows the respective adsorption isotherms plotted as the amount of CO_2 adsorbed on 1 m^2 of the network surface vs. the CO_2 pressure.

The CO_2 adsorption capacities of both non-functionalized P(DEB) and P(DEBPh) networks were about

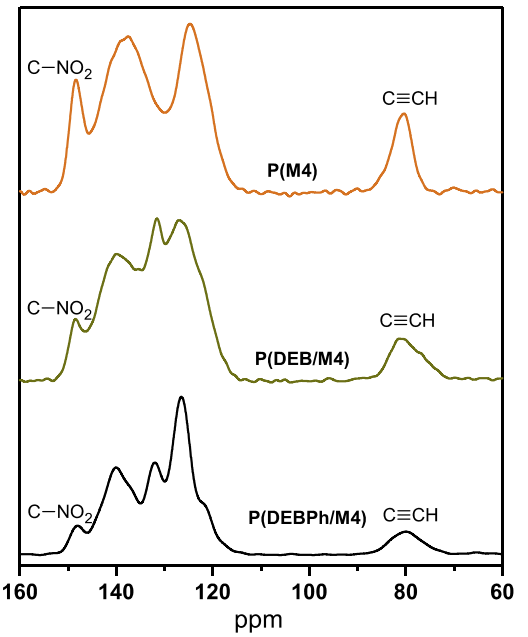

Fig. 5. ^{13}C CP/MAS NMR of polymers of Table 2.

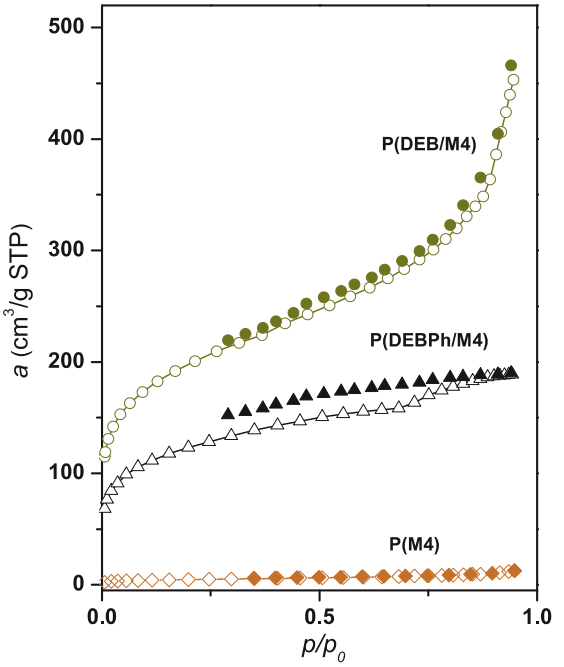

Fig. 6. N_2 adsorption isotherms on polymers of Table 2.

Table 2
Homo and copolymerization of M4. *Y* is the polymer yield, ($x_{LF} + x_{BF}$) is the total mole fraction of the nitro group bearing monomeric units, ($x_{BN} + x_{BF}$) is the total fraction of the branching monomeric units, $c_{(FG)}$ is the content of nitro groups in mmol/g. S_{BET} is the specific surface area, V_T is the total pore volume at $p/p_0 = 0.95$ and $V_{0.1}$ is the pore volume at $p/p_0 = 0.10$ (all from the N_2 adsorption isotherms).

Polymer Code	Monomers	*Y* (%)	$x_{LF} + x_{BF}$	$x_{BN} + x_{BF}$	$c_{(FG)}$ (mmol/g)	S_{BET} (m^2/g)	$V_{0.1}$ (cm^3/g)	V_T (cm^3/g)
P(M4)	M4	85	1.00	0.48	6.5	16	–	0.02
P(DEB/M4)	DEB + M4	88	0.45	0.55	3.1	667	0.27	0.70
P(DEBPh/M4)	DEBPh + M4	90	0.45	0.49	2.4	413	0.17	0.29

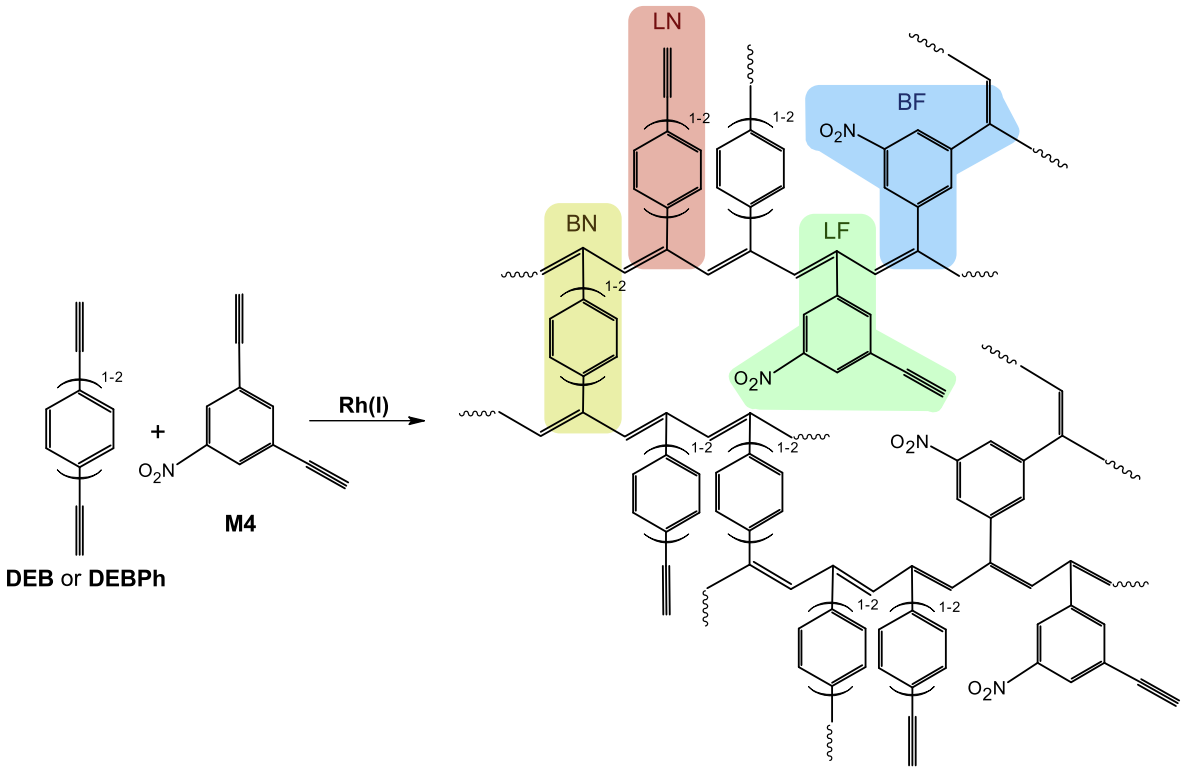

Scheme 3. Monomeric units in copolymers of DEB or DEBPh with 1,3-diethynyl-5-nitrobenzene.

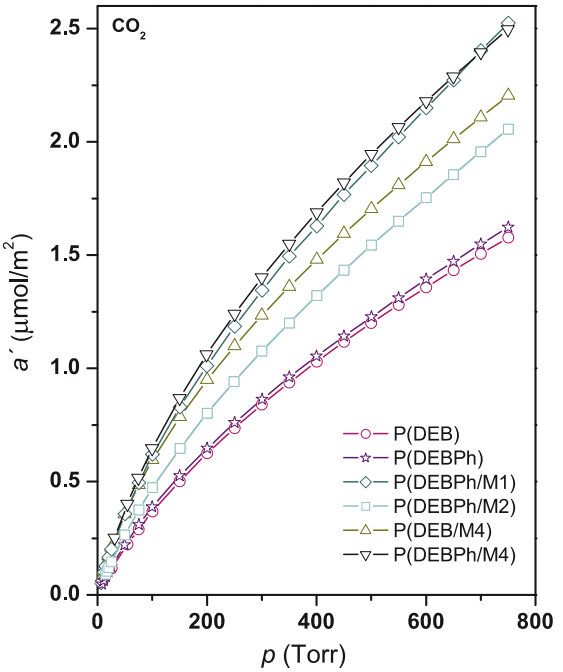

Fig. 7. CO_2 adsorption isotherms (μmol CO_2 adsorbed per 1 m^2 vs. CO_2 pressure) on selected polymers at 273 K.

1.60 μmol/m^2 (at p = 750 Torr). The functionalization of the networks resulted in an enhancement of the CO_2 adsorption capacity to 2.05 μmol/m^2 in the case of CH_2OH containing P(DEBPh/M2) and to values from 2.21 to 2.52 μmol/m^2 in the case of NO_2 containing networks P(DEB/M4), P(DEBPh/M4), and P(DEBPh/M1) (p = 750 Torr). This very probably reflects an enhancement of the interaction energy between CO_2 and the network surface due to the network functionalization. Both (i) (weak) Lewis basicity of the oxygen atoms in NO_2 and OH groups (with respect to CO_2) and (ii) polarization of the phenyl moieties bearing NO_2 or OH groups may contribute to the increase in energy of the CO_2-surface interaction. The increase in CO_2 adsorption capacity is more pronounced for the networks containing NO_2 groups than for the networks with CH_2OH groups. If we take nitrobenzene and (hydroxymethyl)benzene molecules as an approximation to the nitrophenyl and (hydroxymethyl)phenyl groups of the networks, we can state that the last finding correlates well with the trend in dipole moments of nitrobenzene (4.22 D) and (hydroxymethyl)benzene (1.71 D) [47].

3.4. The DR UV/vis spectra and TGA characteristics of prepared polymers

Fig. 8 shows the DR UV/vis spectra of DEB series of polymers of Table 1 (the spectra of the remaining polymers are available in Supplementary Data). The spectra of all the polymers exhibit a broad absorption band in the visible region, which is attributable to the π–π* transition of partially conjugated polyene main chains. The wavelengths of UV/vis absorption maxima (λ_{max}) of non-functionalized networks and networks with NO_2 and CH_2OH groups are

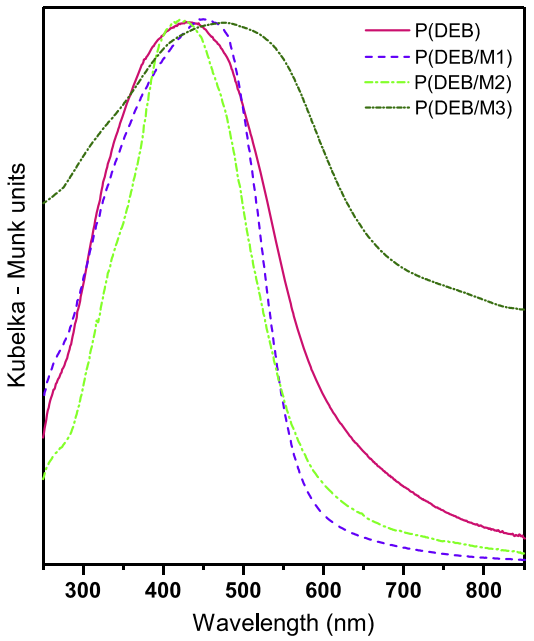

Fig. 8. DR UV/vis spectra of DEB series of polymers of Table 1.

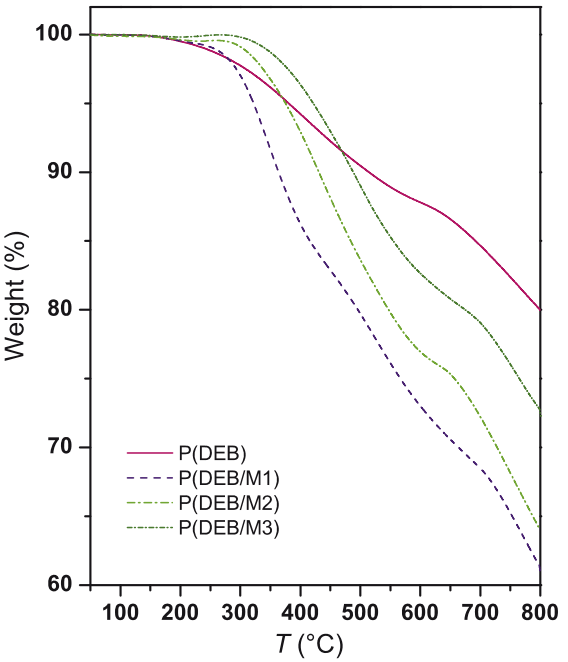

Fig. 9. TGA curves for DEB series of polymers of Table 1.

Table 3
Temperature at which the weight loss upon heating under nitrogen reaches 5%, $t_{95\%}$, weight loss at 800 °C, Δw, and the wavelength of DR UV/vis absorption maxima, λ_{max}, for polymers from Tables 1 and 2. Concentration of functional groups in the polymers, $c_{(FG)}$.

Polymer code	Functional group	$c_{(FG)}$ (mmol/g)	$t_{95\%}$ (°C)	Δw (%); 800 °C	λ_{max} (nm)
P(M4)	NO_2	6.5	291	65.3	425
P(DEB/M1)	NO_2	3.7	320	38.7	435
P(DEB/M4)	NO_2	3.1	317	32.2	400
P(DEBPh/M1)	NO_2	2.5	317	25.5	455
P(DEBPh/M4)	NO_2	2.4	357	22.1	460
P(DEBPh)	None	–	397	18.4	450
P(DEB)	None	–	381	20.0	430
P(DEB/M2)	CH_2OH	3.9	375	35.9	420
P(DEBPh/M2)	CH_2OH	3.0	408	26.4	385
P(DEBPh/M3)	Ph_2N	2.1	448	20.6	475
P(DEB/M3)	Ph_2N	2.0	419	27.2	475

in the interval of 390–460 nm (Table 3). A slight red shift from these values is evident in the polymers containing diphenylamino groups (λ_{max} = 475 nm).

TGA curves for the DEB series of polymers of Table 1 are shown in Fig. 9 (the TGA curves for the remaining polymers are available in Supplementary Data). The values of the temperature at which the weight loss of the polymer upon heating under nitrogen reaches 5% ($t_{95\%}$) are listed in Table 3. If we consider this quantity as the stability criterion, we can conclude that the stability of the polymers increases depending on the functional group as follows: NO_2 < CH_2OH ~ none < Ph_2N. The weight loss (Δw) at 800 °C of all functionalized networks exceeds that of the hydrocarbon P(DEB) and P(DEBPh) networks (Table 3). As expected, the functionalization with nitro groups causes the most pronounced decrease in the thermal stability of the networks. This is most evident in the case of the P(M4) network, which contains the highest concentration of nitro groups.

4. Conclusions

The chain-growth copolymerization of 1:1 mixture of diethynylarenes and monoethynylbenzenes substituted in the *para* position with NO_2, CH_2OH or Ph_2N groups provides high yields of conjugated polyacetylene-type networks with heteroatomic functional groups. The proper selection of the size ratio of (i) the arylene linker of bifunctional monomer and (ii) the pendant group of a monofunctional monomer allows to prepare highly cross-linked networks containing micro- and mesopores and exhibiting a high specific surface area. Particularly, the combinations of 4,4′-diethynylbiphenyl with either 1-ethynyl-4-nitrobenzene or 1-ethynyl-4-(hydroxymethyl)benzene provides networks with S_{BET} of up to 459 m^2/g. Low demand for the number of ethynyl groups per monomer molecule in the feed (average f value = 1.5) and relatively high content of the heteroatomic functional groups in the networks (2.5–3.9 mmol/g) are the main advantages of the described process of preparing porous conjugated networks. The S_{BET} values up to 667 m^2/g are achieved in the networks prepared via copolymerization of 1,3-diethynyl-5-nitrobenzene with 1,4-diethynylbenzene or 4,4′-diethynylbiphenyl (1:1, f = 2). On the other hand, the network prepared via homopolymerization of 1,3-diethynyl-5-nitrobenzene exhibits an S_{BET} value of 16 m^2/g only. The deterioration of the porosity may reflect both steric and electronic effects of NO_2 groups that are present in the network in a too high concentration (6.5 mmol/g). The networks functionalized with NO_2 and CH_2OH groups

exhibit a CO_2 adsorption capacity that is about 38–58% greater than that of the corresponding hydrocarbon networks. This most probably reflects the enhancement of the interaction energy between CO_2 and the network surface due to the network functionalization.

Acknowledgements

Financial support from the Czech Science Foundation (Projects no. 15-09637S) and the Science Foundation of Charles University (S.S. Project No. 574612 B-CH, E.S. Project No. 580214) is gratefully acknowledged. Operational Program Research and Development for Innovations co-funded by the European Regional Development Fund and National Budget of Czech Republic, within the framework of project Centre of Polymer Systems (CZ.1.05/2.1.00/03.0111) is gratefully acknowledged.

Appendix A. Supplementary material

Supplementary data associated with this article can be found, in the online version, at http://dx.doi.org/10.1016/j.eurpolymj.2015.03.070.

References

[1] Wu D, Xu F, Sun B, Fu R, He H, Matyjaszewski K. Design and preparation of porous polymers. Chem Rev 2012;112:3959–4015.
[2] Dawson R, Cooper AI, Adams DJ. Nanoporous organic polymer networks. Prog Polym Sci 2012;37:530–63.
[3] Xu S, Luo Y, Tan B. Recent development of hypercrosslinked microporous organic polymers. Macromol Rapid Commun 2013;34:471–84.
[4] Bunz UHF, Seehafer K, Geyer FL, Bender M, Braun I, Smarsly E, et al. Porous polymers based on aryleneethynylene building blocks. Macromol Rapid Commun 2014;35:1466–96.
[5] Liu Q, Tang Z, Wu M, Zhou Z. Design, preparation and application of conjugated microporous polymers. Polym Int 2014;63:381–92.
[6] Germain J, Fréchet JMJ, Švec F. Nanoporous polymers for hydrogen storage. Small 2009;10:1098–111.
[7] Sekizkardes AK, Altarawneh S, Kahveci Z, İslamoğlu T, El-Kaderi HM. Highly selective CO_2 capture by triazine-based benzimidazolelinked polymers. Macromolecules 2014;47:8328–34.
[8] Dawson R, Cooper AI, Adams DJ. Chemical functionalization strategies for carbon dioxide capture in microporous organic polymers. Polym Int 2013;62:345–52.
[9] Li A, Sun H-X, Tan D-Z, Fan W-J, Wen S-H, Qing X-J, et al. Superhydrophobic conjugated microporous polymers for separation and adsorption. Energy Environ Sci 2011;4:2062–5.
[10] Wang J, Wang G, Wang W, Zhang Z, Liu Z, Hao Z. Hydrophobic conjugated microporous polymer as a novel adsorbent for removal of volatile organic compounds. J. Mater. Chem. A 2014;2:14028–37.
[11] Xie Z, Wang C, deKrafft KE, Lin W. Highly stable and porous cross-linked polymers for efficient photocatalysis. J Am Chem Soc 2011;133:2056–9.
[12] Merino E, Verde-Sesto E, Maya EM, Corma A, Iglesias M, Sánchez F. Mono-functionalization of porous aromatic frameworks to use as compatible heterogeneous catalysts in one-pot cascade reactions. Appl. Catal., A 2014;469:206–12.
[13] Thomas A, Kuhn P, Weber J, Titirici M-M, Antonietti M. Porous polymers: enabling solutions for energy applications. Macromol Rapid Commun 2009;30:221–36.
[14] Zhang P, Wu K, Guo J, Wang C. From hyperbranched polymer to nanoscale CMP (NCMP): improved microscopic porosity, enhanced light harvesting, and enabled solution processing into white-emitting Dye@NCMP films. ACS Macro Lett 2014;3:1139–44.
[15] Brandt J, Schmidt J, Thomas A, Epping JD, Weber J. Tunable absorption and emission wavelength in conjugated microporous polymers by copolymerization. Polym Chem 2011;2:1950–2.
[16] Ren S, Dawson R, Adams DJ, Cooper AI. Low band-gap benzothiadiazole conjugated microporous polymers. Polym Chem 2013;4:5585–90.
[17] McKeown NB, Budd PM. Exploitation of intrinsic microporosity in polymer-based materials. Macromolecules 2010;43:5163–76.
[18] Yuan S, Dorney B, White D, Kirklin S, Zapol P, Yu L, et al. Microporous polyphenylenes with tunable pore size for hydrogen storage. Chem Commun 2010;46:4547–9.
[19] Zukal A, Slováková E, Balcar H, Sedláček J. Polycyclotrimers of 1,4-diethynylbenzene, 2,6-diethynylnaphthalene, and 2,6-diethynylanthracene: preparation and gas adsorption properties. Macromol Chem Phys 2013;214:2016–26.
[20] Jiang J-X, Su F, Niu H, Wood HCD, Campbell NL, Khimyak YZ, et al. Conjugated microporous poly(phenylene butadiynylene)s. Chem Commun 2008:486–8.
[21] Wu K, Guo J, Wang C. Gelation of metalloporphyrin-based conjugated microporous polymers by oxidative homocoupling of terminal alkynes. Chem Mater 2014;26:6241–50.
[22] Jiang X, Su F, Trewin A, Wood CD, Campbell NL, Niu H, et al. Conjugated microporous poly(aryleneethynylene) networks. Angew Chem Int Ed 2007;46:8574–8.
[23] Holst JR, Stöckel E, Adams DJ, Cooper AI. High surface area networks from tetrahedral monomers: metal-catalyzed coupling, thermal polymerization, and "click" chemistry. Macromolecules 2010;43:8531–8.
[24] Wang Z, Yuan S, Mason A, Reprogle B, Liu D-J, Yu L. Nanoporous porphyrin polymers for gas storage and separation. Macromolecules 2012;45:7413–9.
[25] Plietzsch O, Schilling CI, Grab T, Grage SL, Ulrich AS, Comotti A, et al. Click chemistry produces hyper-cross-linked polymers with tetrahedral cores. New J Chem 2011;35:1577–81.
[26] Xu Y, Jin S, Xu H, Nagai A, Jiang D. Conjugated microporous polymers: design, synthesis and application. Chem Soc Rev 2013;42:8012–31.
[27] Zhang Y, Zhang Y, Sun YL, Du X, Shi JY, Wang WD, et al. 4-(N,N-dimethylamino)pyridine-embedded nanoporous conjugated polymer as a highly active heterogeneous organocatalyst. Chem Eur J 2012;18:6328–34.
[28] Jiang JX, Wang C, Laybourn A, Hasell T, Clowes R, Khimyak YZ, et al. Metal-organic conjugated microporous polymers. Angew Chem Int Ed 2011;50:1072–5.
[29] Zhang P, Weng Z, Guo J, Wang C. Solution-dispersible, colloidal, conjugated porous polymer networks with entrapped palladium nanocrystals for heterogeneous catalysis of the Suzuki–Miyaura coupling reaction. Chem Mater 2011;23:5243–9.
[30] Dawson R, Laybourn A, Clowes R, Khimyak YZ, Adams DJ, Cooper AI. Functionalized conjugated microporous polymers. Macromolecules 2009;42:8809–16.
[31] Guillerm V, Weselinski LJ, Alkordi M, Mohideen MIH, Belmabkhout Y, Cairns AJ, et al. Porous organic polymers with anchored aldehydes: a new platform for post-synthetic amine functionalization en route for enhanced CO_2 adsorption properties. Chem Commun 2014;50:1937–40.
[32] Bildirir H, Paraknowitsch JP, Thomas A. A tetrathiafulvalene (TTF)-conjugated microporous polymer network. Chem Eur J 2014;20:9543–8.
[33] Ma HP, Ren H, Zou XQ, Meng S, Sun FX, Zhu GS. Post-metalation of porous aromatic frameworks for highly efficient carbon capture from $CO_2 + N_2$ and $CH_4 + N_2$ mixtures. Polym Chem 2014;5:144–52.
[34] Ratvijitvech T, Dawson R, Laybourn A, Khimyak YZ, Adams DJ, Cooper AI. Post-synthetic modification of conjugated microporous polymers. Polymer 2014;55:321–5.
[35] Kiskan B, Weber J. Versatile postmodification of conjugated microporous polymers using thiol-yne chemistry. ACS Macro Lett 2012;1:37–40.
[36] Cho HC, Lee HS, Chun J, Lee SM, Kim HJ, Son SU. Tubular microporous organic networks bearing imidazolium salts and their catalytic CO_2 conversion to cyclic carbonates. Chem Commun 2011;47:917–9.
[37] Hanková V, Slováková E, Zedník J, Vohlídal J, Sivkova R, Balcar H, et al. Polyacetylene-type networks prepared by coordination polymerization of diethynylarenes: new type of microporous organic polymers. Macromol Rapid Commun 2012;33:158–63.
[38] Lavastre O, Cabioch S, Dixneuf PH, Sedláček J, Vohlídal J. New route to conjugated polymer networks: synthesis of poly(4-ethynyl)phenylacetylene and its transformation into a conjugated network. Macromolecules 1999;32:4477–81.
[39] Shiotsuki M, Sanda F, Masuda T. Polymerization of substituted acetylenes and features of the formed polymers. Polym Chem 2011;2:1044–58.

[40] Bondarev D, Zedník J, Plutnarová I, Vohlídal J, Sedláček J. Molecular weight and configurational stability of poly[(fluorophenyl) acetylene]s prepared with metathesis and insertion catalysts. J Polym Sci Polym Chem 2010;48:4296–309.
[41] Slováková E, Zukal A, Brus J, Balcar H, Brabec L, Bondarev D, et al. Transition-metal-catalyzed chain-growth polymerization of 1,4-diethynylbenzene into microporous crosslinked poly (phenylacetylene)s: the effect of reaction conditions. Macromol Chem Phys 2014;215:1855–69.
[42] Slováková E, Ješelnik M, Žagar E, Zedník J, Sedláček J, Kovačič S. Chain-growth insertion polymerization of 1,3-diethynylbenzene high internal phase emulsions into reactive π-conjugated foams. Macromolecules 2014;47:4864–9.
[43] Trhlíková O, Zedník J, Balcar H, Brus J, Sedláček J. [Rh (cycloolefin)(acac)] complexes as catalysts of polymerization of aryl-and alkylacetylenes: influence of cycloolefin ligand and reaction conditions. J Mol Catal A: Chem 2013;378:57–66.
[44] Mastrorilli P, Nobile CF, Rizzuti A, Suranna GP, Acierno D, Amendola E. Polymerization of phenylacetylene and of *p*-tolylacetylene catalyzed by β-dioxygenato rhodium(I) complexes in homogeneous and heterogeneous phase. J Mol Catal A: Chem 2002;178:35–42.
[45] Dušek K, Dušková-Smrčková M. Network structure formation during crosslinking of organic coating systems. Progr Polym Sci 2000;25:1215–60.
[46] Hamzehlou S, Reyes Y, Leiza JR. A new insight into the formation of polymer networks: a kinetic Monte Carlo simulation of the cross-linking polymerization of S/DVB. Macromolecules 2013;46:9064–73.
[47] Nelson Jr RD, Lide Jr DR, Maryott A. National standard reference data series – National bureau of standards 10, vol. 10. Washington, D.C.: U.S. Government Printing Office; 1967.